Seismic Oceanography; A tomographic reconstruction of a two-dimensional flowing medium

Bachelor Thesis	:	Jip van Steen
Student number	:	3761916
Date	:	June 10, 2016
Supervisor	:	dr. Tristan van Leeuwen

University of Utrecht
Faculty of Science
Mathematics & Applications

Abstract

The flow velocity varies throughout the ocean. Seismic techniques (the transmittance and interception of seismic waves to acquire data) can be used to image the two-dimensional velocity field of the ocean. A finite difference method, which is based on fluid mechanics, can be used to model seismic wave-propagation in homogeneous and inhomogeneous flowing media. The numerical implementation of this finite difference method will be illustrated in *Matlab*. By measuring the changing of various parameters at a certain level in the ocean, seismic waves can be observed. In this study, the changing of the parameter pressure is focused on. By creating synthetic measurements (self-created measurements with a known velocity field), the aim is to determine the velocity field out of these measurements. This can generally be achieved by matching simulations to the synthetic measurements, followed by an inverse procedure. This inverse procedure will be discussed and demonstrated, considering homogeneous flowing media. The difficulties that come along when considering more realistic scenarios are discussed.

Contents

1 Introduction

Oceanography, also known as oceanology, is in general the study of the ocean. It covers a wide and diverse range of topics. Marine life and ecosystems, the chemical properties of the ocean, ocean circulation, plate tectonics and the geology of the seafloor are some examples of topics covered by oceanography. The collective aim of all these topics is to get a better understanding of the global ocean and the processes within. In order to efficiently group the wide range of topics, oceanography is divided into various disciplines. The major disciplines within the oceanography are geological oceanography, physical oceanography and chemical oceanography. A relatively new field of research within oceanography is seismic oceanography.

Seismic oceanography investigates structures in the ocean by means of seismic imaging. Seismic imaging is a tool that investigates the subsurface with the use of sound waves, also termed seismic waves (both terms will be used interchangeably throughout this study, meaning exactly the same thing). In 2003, a research group led by W. Steven Holbrook discovered that with the use of seismic reflection techniques, information about the interior of the ocean could be mapped out and illustrated. This technique had been used in the past to image the solid earth beneath the ocean, but it was found that this technique also provided a lot of detailed information about the ocean itself. The research group presented their findings of of the explored area of the ocean interior in a paper published in Science [Holbrook et al., 2003]. They showed that distinct water masses (water masses with different pressures and temperatures) can be mapped and their internal structures imaged. It had therefore been shown that with the use of seismic reflection techniques, important oceanic phenomena can be imaged with great detail.

Since this discovery, more studies with this new tool have been done to explore the many possibilities seismic oceanography has to offer. By observing the changing speed of sound waves propagating through the ocean, oceanographers hope to extract information about the ocean's temperature, salinity and velocity. This study will focus on extracting the velocity field of the ocean with the help of seismic imaging. In this study a two-dimensional ocean intersection is considered.

In order to extract the velocity field out of emitting and observing seismic waves, one first needs to know how a seismic wave propagates through a medium such as the ocean. This process can be described by valid fluid dynamics equations. By constructing a model of an ocean intersection, this process can be simulated by means of (numerically) implementing these equations into the model. It is therefore possible to simulate the propagation of a seismic wave through the ocean intersection, including potential reflections.

Seismic waves can be observed at a certain observance location by measuring various parameters. If the process of propagation of a seismic wave through the ocean can be simulated, the parameters that would be measured at this observance location can be simulated as well. Therefore, the measurements done to detect a passing sound wave at the observation point can be simulated.

The aim of this study is to determine the velocity flow field of the two-dimensional ocean intersection by means of seismic imaging. With the help of simulating the process of sound wave propagation through the ocean intersection, simulated measurements can be created for a specific velocity field. By matching these simulations to the synthetic measurements, which are self-constructed under the assumption that the velocity field is unknown, it will be attempted to extract the velocity field. This inverse procedure will be illustrated and discussed in this study.

2 Definitions

In this study, various mathematical terms will be discussed. To avoid repetitions and redundancy, an introduction section with the used definitions in this study is necessary. All the non-trivial mathematical terms used in this study are discussed here in this section.

Because this study focuses on the velocity field in two dimensions of an intersection of the ocean, the third dimension is ignored. Therefore a two-dimensional Cartesian coordinate system is considered throughout this study.

In order to clarify that a certain variable a is a vector, the variable will be denoted in bold : $\mathbf{a} = (a_x, a_y)$. The nabla-symbol used in this study is defined and denoted as: $\nabla := (\partial/\partial x, \partial/\partial y)$. The nabla can be used as an operator, as well as to determine the gradient and the divergence, depending on the notation.

For clarification, assume a pressure function $P(x, y) \in \mathbb{R}$ and a vector velocity function $\mathbf{v} = (v_x, v_y) \in \mathbb{R}^2$ exists in a two-dimensional Cartesian coordinate system. The gradient of only scalar-valued functions can be determined, so the gradient of only P can be determined. This is denoted as follows:

$$grad(P) = \nabla P = \left(\frac{\partial P}{\partial x}, \frac{\partial P}{\partial y}\right).$$

The divergence is denoted as the dot-product between the nabla-symbol and the certain vector. Therefore, the divergence of the pressure is denoted as follows:

$$div(P) = \nabla \cdot P = \frac{\partial P}{\partial x} + \frac{\partial P}{\partial y}.$$

Though the notation of the divergence looks very similar to the notation of the gradient, it should be denoted with great care. The gradient can only be taken from a scalar-valued function, while the divergence does not have this constraint. Therefore the gradient of the vector velocity cannot be determined (because $\mathbf{v}$ is a vector), while the divergence of the vector velocity can be calculated as follows:

$$div(\mathbf{v}) = \nabla \cdot \mathbf{v} = \nabla \cdot (v_x, v_y)^T = \frac{\partial v_x}{\partial x} + \frac{\partial v_y}{\partial y}.$$

Another notation which is also mentioned in this study is the dot-product of a vector and the nabla, which is not the same as the divergence of a vector. This is noted as follows:

$$\mathbf{v} \cdot \nabla = v_x \cdot \frac{\partial}{\partial x} + v_y \cdot \frac{\partial}{\partial y}.$$

Furthermore, the Frobenius norm will be used later on in this study. Suppose X as a $(m \times n)$-matrix with elements x_{ij}; $0 \leq i \leq m$, $0 \leq j \leq n$ with $i, j, m, n \in \mathbb{N}$ $(i < m, j < n)$. Then X looks like:

$$X = \begin{pmatrix} x_{00} & x_{01} & \dots & x_{0n} \\ x_{10} & x_{11} & \dots & x_{1n} \\ \vdots & \vdots & \ddots & \vdots \\ x_{m0} & x_{m1} & \dots & x_{mn} \end{pmatrix}.$$

The Frobenius norm, sometimes also called the Euclidean norm, on X is then defined as:

$$||X||_F := \left(\sum_{i=0}^{m} \sum_{j=0}^{n} |x_{ij}|^2 \right)^{1/2}, \tag{1}$$

which is the square root of the sum of the squares of its elements.

Lastly, Taylor's theorem will be of use. Especially the k'th order Taylor polynomial with its remainder term. This is stated as follows:

Theorem 2.1 *Let $k \geq 1$ be an integer and let the function $f : \mathbb{R} \to \mathbb{R}$ be k-times differentiable at the point $a \in \mathbb{R}$. Then the k'th order of the polynomial appearing in Taylor's theorem is stated as:*

$$P_k(x) = f(a) + (x-a)f'(a) + (x-a)^2 \frac{f''(a)}{2!} + \cdots + (x-a)^k \frac{f^{(k)}(a)}{k!}, \tag{2}$$

of the function f at the point a. Taylor's theorem describes the behavior of the remainder term as:

$$R_k(x) = f(x) - P_k(x) = (x-a)^{k+1} \frac{f^{(k+1)}(\xi_L)}{(k+1)!}, \tag{3}$$

for some real number ξ_L between a and x.

This theorem is assumed to be known to the reader, but [Vuik et al., 2006] is referred to for further insight.

3 Introduction seismic oceanography

For decades, seismic waves have been used to study the earth beneath the ocean floor. With the help of hydrophones (microphones designed for underwater recording) towed behind a ship, sound waves can be emitted and intercepted to acquire useful data about the earth beneath the ocean. These sound waves are (partly) reflected due to the different layers in the earth. Therefore, the emittance, the reception and the travel time in between gives useful information about what kind of materials lay beneath the ocean.

Seismic oceanography uses the same reflection-technique, but focuses on the imaging of the structures within the ocean interior instead of the earth beneath the ocean [Ruddick et al., 2009]. In this section, the basic principles of seismic oceanography are discussed within the context of relevance for this study and with the primary aim of determining the velocity field out of the reflection and interception of seismic waves.

As said, an array of hydrophones towed by a ship floating in the ocean can emit and receive seismic waves. A sketch made to illustrate this is shown in figure 1. To get proper data, the amount of hydrophones is usually very high, resulting in a rope of hydrophones which is often several kilometers long [Ruddick et al., 2009]. The hydrophones are towed at usually about 15 meters beneath the water surface. The sound waves emitted from the hydrophones can be reflected by so called reflectors. Seismic waves can be reflected in the ocean by changes in the acoustic impedance. The acoustic impedance is defined as density times the sound velocity. Fortunately, the oceanic reflectors are mostly horizontal, resulting in the strongest reflections.

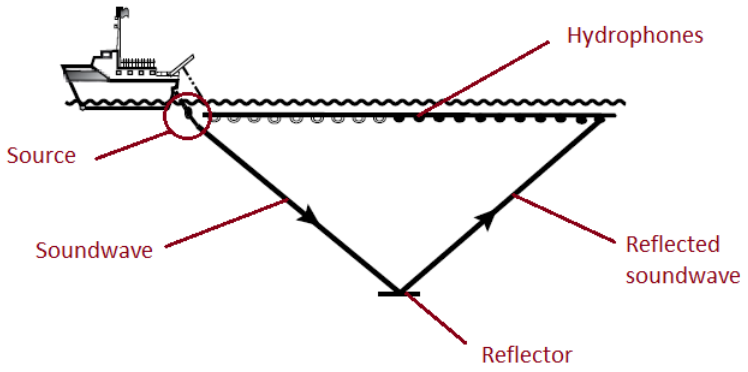

Figure 1: Sketch.

In this study, the determination of the velocity field is of primary concern. Locating the structures within the ocean that reflect due to changes in acoustic impedance is another branch in the seismic oceanography and will therefore be ignored.

For the implementation of the wave-propagation later on, it is important to state some assumptions beforehand, to simplify the problem. Firstly, it will be assumed that one of the hydrophones (or the ship itself) sends out the seismic waves and the hydrophones lay perfectly on a horizontal line at some distance beneath the water-surface. Secondly it will be assumed that there is only one oceanic reflector at a certain depth, the ocean floor, which is parallel to the water-surface. Therefore, the seismic waves will bounce back from the reflector, reaching the hydrophones again in time (see figure 1). Note that the seismic wave does not only travel from the source along the arrow, but travels naturally in all directions. This figure is merely to show the process of reflection.

Now that the context for the model has been constructed, the hydrophones can detect the direct and reflected seismic waves that are passing through at their location. The seismic waves can be observed by measuring various parameters. Because sound is merely a repeating pattern of high and low pressure regions that propagates through a medium (sometimes also called a pressure wave), the pressure is the most common/logical parameter to be measured at the hydrophones.

The other parameters that can be observed are the so called acoustic velocity components (w_x,w_y). This is the change in velocity at a certain point due to a passing sound wave. It is not unimaginable that these parameters are measured, but it is unlikely to be observed in practice because the change in acoustic velocity due to a propagating wave is far smaller than the change in pressure due to the same wave.

So because the pressure is most common to be measured at the hydrophones, this study will focus on measurements based on the observance of pressure through time. This leaves the question of how to determine the velocity field of this two-dimensional intersection by means of these pressure measurements at the hydrophones.

Assume the hydrophones kept a record of the pressure between a certain start time, and a certain end time. These are called the measurements. To determine the velocity field out of these observed measurements, one can try to simulate the situation for a specific velocity field and compile the (simulated) measurements for this case. After that, the real measurements can be compared with the simulated measurements. If they are almost identical, the velocity fields will also be close to each other. This comparison can be done for a lot of different velocity fields, (thus, a lot of simulated measurements can be compared with the real measurements) and one can determine which simulation is the closest to the real measurements.

The whole process of trying to find the velocity field out of matching the simulations with the measurements is called an inverse procedure. This procedure will be shown and discussed in detail later on. Because there is no data available in studies, synthetic measurements will be created to show this inverse procedure. However, before this procedure can start, one needs to know what fluid dynamics equations can describe a medium like the ocean including the propagation of a sound wave through it.

4 Fluid dynamics equations

The equations of the fluid dynamics in a certain medium (e.g. water or air) can be simplified into various simpler sets. In this study, one specific set will be discussed and analysed with the help of *Matlab*. But before the fluid dynamics equations can be discussed, the involved variables will be defined first.

The Cartesian coordinates are defined as $\mathbf{R} = (x, y)$, and the time is denoted with t. For a specific point in the medium at a certain time, the following variables can be determined: $\bar{P}(\mathbf{R}, t)$ stands for the pressure, $\bar{\varrho}(\mathbf{R}, t)$ is the density, $\bar{\mathbf{v}}(\mathbf{R}, t)$ is the velocity vector and $\bar{S}(\mathbf{R}, t)$ is the entropy in a medium. These four variables may vary throughout the medium and depend on the time.

A complete set of fluid dynamic equations is adopted from [Ostashev et al., 2005]. These are the most basic equations for describing the medium (with potentially a seismic wave passing through). The detailed origin of this set is discussed in [Ostashev et al., 2005].

$$\left(\frac{\partial}{\partial t} + \bar{\mathbf{v}} \cdot \nabla\right) \bar{\mathbf{v}} + \frac{\nabla \bar{P}}{\bar{\varrho}} - \mathbf{g} = \frac{\mathbf{F}}{\bar{\varrho}}, \tag{4}$$

$$\left(\frac{\partial}{\partial t} + \bar{\mathbf{v}} \cdot \nabla\right) \bar{\varrho} + \bar{\varrho} \nabla \cdot \bar{\mathbf{v}} = \bar{\varrho} Q, \tag{5}$$

$$\left(\frac{\partial}{\partial t} + \bar{\mathbf{v}} \cdot \nabla\right) \bar{S} = 0, \tag{6}$$

$$\bar{P} = \bar{P}(\bar{\varrho}, \bar{S}). \tag{7}$$

In this set, g represents the acceleration due to the gravity, $\mathbf{F}$ represents a force acting on the medium and Q characterizes a mass source. They are considered to be constant.

In the absence of a sound wave propagating through the medium, the pressure, the density, the velocity vector and the entropy are equivalent to their ambient values P, ϱ, $\mathbf{v}$ and S (without the bars on top). Though in the presence of a propagating wave, the fluctuations caused by the propagating wave begin to matter. Therefore, if a seismic wave moves through a medium, these variables can be expressed in their ambient values plus their fluctuation values p, η, $\mathbf{w}$ and s. Note that $\mathbf{w} = (w_x, w_y)$ stands for the acoustic velocity (mentioned previously). This gives the following set of variables:

$$\begin{cases} \bar{P} &= P + p, \\ \bar{\varrho} &= \varrho + \eta, \\ \bar{\mathbf{v}} &= \mathbf{v} + \mathbf{w}, \\ \bar{S} &= S + s. \end{cases}$$

So in order to account for the fluctuations due to the propagating wave, the bar is placed on top of the variables.

In order to obtain the equations for a sound wave propagating through a medium, the equations (4)-(7) can be transformed to another equation set under the main restraint that a sound wave is generated by the mass source Q and a force $\mathbf{F}$. The newly derived equation set shows that the fluctuation values p, η, $\mathbf{w}$ and s can be calculated if the ambient quantities ϱ, $\mathbf{v}$, P, S, c and h are known. Where c is the adiabatic sound speed and h is given. This new equation set is known to be the most general description of sound-wave propagation in a moving inhomogeneous medium. However, because this set is not of major importance in this study, the reader is therefore referred to [Ostashev et al., 2005] for further detail on this equation set.

Two specific equations can be derived out of this transformed version of equations set (4)-(7) (with a lot of steps in between, shown in [Ostashev et al., 2005]). This results in equations:

$$\frac{dp}{dt} + \varrho c^2 \nabla \cdot \mathbf{w} + \mathbf{w} \cdot \nabla P + \left(\varrho\beta\eta + c^2(1 - \alpha\varrho/h)\eta + (\alpha\varrho/h)p\right) \nabla \cdot \mathbf{v} = \varrho c^2 Q, \quad (8)$$

and

$$\frac{d\mathbf{w}}{dt} + (\mathbf{w} \cdot \nabla)\mathbf{v} + \frac{\nabla p}{\varrho} - \frac{\eta \nabla P}{\varrho^2} = \frac{\mathbf{F}}{\varrho}. \quad (9)$$

This equation set is of importance, because out of these equations, two coupled equations can be derived which will be the basis of the model discussed in this study.

5 A usable equation set

Out of the fluid dynamics equations discussed in the previous section, two coupled usable equations can be derived. However, to make this possible, three important restrictions and approximations have to be taken into account as they were used to derive these equations:

1. The speed of sound is not the same in all substances. Sound travels about four times faster through water than it does through air. Therefore it can be assumed that the magnitude of the velocity-vector is always much less than the sound speed in the ocean ($|\mathbf{v}| \ll c$).

2. With the help of [Landau and Sykes, 1987] and [Ostashev et al., 2005], it can be shown that in equation (8) the term proportional to $\nabla \cdot \mathbf{v}$ can be ignored.

3. Furthermore, in both (8) and (9), the terms proportional to $\nabla \cdot P$ can also be ignored because the ambient pressure is assumed to be constant (and therefore $\nabla \cdot P = 0$).

4. And last, the full derivative with respect to time is introduced and defined as: $\frac{d}{dt} = \frac{\partial}{\partial t} + \mathbf{v} \cdot \nabla$.

Using these four notes, equation set (8) and (9) are transformed into

$$\left(\frac{\partial}{\partial t} + \mathbf{v} \cdot \nabla\right) p + \varrho c^2 \nabla \cdot \mathbf{w} = \varrho c^2 Q, \quad (10)$$

$$\left(\frac{\partial}{\partial t} + \mathbf{v}\cdot\nabla\right)\mathbf{w} + (\mathbf{w}\cdot\nabla)\mathbf{v} + \frac{\nabla p}{\varrho} = \mathbf{F}/\varrho. \tag{11}$$

Equations (10) and (11) are also derived in [Ostashev, 1987] using a different approach. This equation set is applicable for sound propagation through moving inhomogeneous media (gasses or liquids) and is therefore also applicable for the ocean.

This coupled set can be used to calculate the pressure (p) and the acoustic velocity ($\mathbf{w}$) through time. In order to solve this set, the ambient quantities: speed of sound (c), the density (ϱ) and the velocity ($\mathbf{v}$) need to be known. This set will be modeled to simulate wave propagation through the two-dimensional ocean intersection. The numerical implementation will be discussed in the next section. In addition, because a lot of terms are ignored and a lot of assumptions have been made to construct this equation set (10) and (11), the applicability of this equation set will be studied.

Several cases for the velocity field will be considered, a non-moving medium, a homogeneous moving medium and a heterogeneous moving medium. The equations for these situations need to be transformed in such a way that the pressure and the acoustic velocity derivatives can be calculated (should be on the left hand side). This makes them easy to implement in the next section.

5.1 Non-moving medium

First, consider an ocean that has no movement at all ($\mathbf{v} = 0$). This means that all the terms proportional to $\mathbf{v}$ can be neglected. After some simple transformations, the equations (10) and (11) become:

$$\frac{\partial p}{\partial t} = \varrho c^2 \left(Q - \nabla\cdot\mathbf{w}\right), \tag{12}$$

$$\frac{\partial w_x}{\partial t} = \left(F_x - \frac{\partial p}{\partial x}\right)/\varrho, \tag{13}$$

$$\frac{\partial w_y}{\partial t} = \left(F_y - \frac{\partial p}{\partial y}\right)/\varrho. \tag{14}$$

It is shown in [Ostashev et al., 2005] that for a non-moving medium, the set of fluid dynamics equations (4)-(7) can also be exactly reduced to a single equation:

$$\frac{\partial}{\partial t}\left(\frac{1}{\varrho c^2}\frac{\partial p}{\partial t}\right) - \nabla\cdot\left(\frac{\nabla p}{\varrho}\right) = 0, \tag{15}$$

which coincides with equation set (12), (13), (14).

5.2 Homogeneous uniformly moving medium

In the case of a homogeneous uniformly moving medium, the ambient quantities do not depend on their position or the time. This means that the variables c, $\mathbf{v}$, ϱ are constant throughout the medium and throughout the time. Likewise, the (partial) derivatives of $\mathbf{v}$ with respect to time and space are zero. Thus, equation set (10) and (11) are transformed into:

$$\frac{\partial p}{\partial t} = -(\mathbf{v} \cdot \nabla)p + \varrho c^2(Q - \nabla \cdot \mathbf{w}), \tag{16}$$

$$\frac{\partial w_x}{\partial t} = -(\mathbf{v} \cdot \nabla)w_x + \left(F_x - \frac{\partial p}{\partial x}\right)/\varrho, \tag{17}$$

$$\frac{\partial w_y}{\partial t} = -(\mathbf{v} \cdot \nabla)w_y + \left(F_y - \frac{\partial p}{\partial y}\right)/\varrho. \tag{18}$$

It is shown in [Ostashev et al., 2005] that for a homogeneously moving medium, the equation set (4)-(7) can also be exactly reduced to a single equation:

$$\left(\frac{\partial}{\partial t} + \mathbf{v} \cdot \nabla\right)^2 p - c^2 \nabla^2 p = 0, \tag{19}$$

which coincides with equation set (16), (17), (18).

5.3 Heterogeneous moving medium

For a heterogeneous flowing medium, two cases can be subdivided. For each case, a set of equations can be derived having its own equations. In the first case, a stratified moving medium is assumed, where the ambient quantities c, ϱ and $\mathbf{v}$ only depend on the depth (the y-axis). In the second case a turbulent medium is assumed, with temperature and velocity changes throughout the medium. As one can imagine, these are both complex situations resulting in complex equations. Both are described and illustrated in [Ostashev et al., 2005].

The conclusion in [Ostashev et al., 2005] is that these newly derived equations for the stratified moving medium correspond exactly with the equation set (10) and (11). The same goes for the turbulent moving medium, under some approximations. Therefore, the equations (10) and (11) cannot further be simplified, yielding the following three equations for a heterogeneous flowing medium:

$$\frac{\partial p}{\partial t} = -(\mathbf{v} \cdot \nabla)p + \varrho c^2(Q - \nabla \cdot \mathbf{w}), \tag{20}$$

$$\frac{\partial w_x}{\partial t} = -(\mathbf{v} \cdot \nabla)w_x - (\mathbf{w} \cdot \nabla)v_x + \left(F_x - \frac{\partial p}{\partial x}\right)/\varrho, \tag{21}$$

$$\frac{\partial w_y}{\partial t} = -(\mathbf{v} \cdot \nabla)w_y - (\mathbf{w} \cdot \nabla)v_y + \left(F_y - \frac{\partial p}{\partial y}\right)/\varrho. \tag{22}$$

Thus (10) and (11) describe wave propagation exactly through a non-moving and a homogeneously moving medium. And using some assumptions, it can also describe wave propagation through heterogeneous moving medium. Therefore, the validity of this equation set has been checked and it can now be implemented in the model.

With the help of *Matlab*, wave propagation through the two-dimensional medium can be simulated using equations (10) and (11) (or its discussed variants, depending on what kind of flowing medium is assumed).

6 Implementation in *Matlab*

In order to model the wave-propagation in a flowing medium, a finite difference method will be used to implement the discussed equation set, consisting of equations (10) and (11). In these equations the third dimension is ignored because the flow field is only considered in the two spatial dimensions x and y, when an intersection of the ocean is investigated. A new set of equations can be derived by transforming equations (10) and (11).

The mass buoyancy $b = 1/\varrho$ and the adiabatic bulk modulus $\kappa = \varrho c^2$ will be used and helpful in the equations below. Equation (10) and (11) then become:

$$\left(\tfrac{\partial}{\partial t} + \mathbf{v} \cdot \nabla\right) p + \kappa \nabla \cdot \mathbf{w} = \kappa Q,$$

$$\left(\tfrac{\partial}{\partial t} + \mathbf{v} \cdot \nabla\right) \mathbf{w} + (\mathbf{w} \cdot \nabla)\mathbf{v} + b\nabla p = b\mathbf{F}.$$

Rewriting these equations with the use of the definition of the gradient and the divergence gives:

$$\frac{\partial p}{\partial t} + \left(v_x \cdot \frac{\partial}{\partial x} + v_y \cdot \frac{\partial}{\partial y}\right) p + \kappa \left(\frac{\partial w_x}{\partial x} + \frac{\partial w_y}{\partial y}\right) = \kappa Q,$$

$$\frac{\partial \mathbf{w}}{\partial t} + \left(v_x \cdot \frac{\partial}{\partial x} + v_y \cdot \frac{\partial}{\partial y}\right) \mathbf{w} + \left(w_x \cdot \frac{\partial}{\partial x} + w_y \cdot \frac{\partial}{\partial y}\right) \mathbf{v} + b\left(\frac{\partial p}{\partial x} + \frac{\partial p}{\partial y}\right) = b\mathbf{F}.$$

In the first equation, the partial derivative with respect to the time can be isolated. The second equation is split into two by using the components along the axes of $\mathbf{w} = (w_x, w_y)$, $\mathbf{v} = (v_x, v_y)$ and the rest of the vectors. After that, the partial derivative in the two dimensions with respect to time can be isolated separately as well. This transformation of the two equations results in the following new equation set:

$$\frac{\partial p}{\partial t} = -\left(v_x \cdot \frac{\partial}{\partial x} + v_y \cdot \frac{\partial}{\partial y}\right) p - \kappa \left(\frac{\partial w_x}{\partial x} + \frac{\partial w_y}{\partial y}\right) + \kappa Q, \tag{23}$$

$$\frac{\partial w_x}{\partial t} = -\left(v_x \cdot \frac{\partial}{\partial x} + v_y \cdot \frac{\partial}{\partial y}\right) w_x - \left(w_x \cdot \frac{\partial}{\partial x} + w_y \cdot \frac{\partial}{\partial y}\right) v_x - b\frac{\partial p}{\partial x} + bF_x, \tag{24}$$

$$\frac{\partial w_y}{\partial t} = -\left(v_x \cdot \frac{\partial}{\partial x} + v_y \cdot \frac{\partial}{\partial y}\right) w_y - \left(w_x \cdot \frac{\partial}{\partial x} + w_y \cdot \frac{\partial}{\partial y}\right) v_y - b\frac{\partial p}{\partial y} + bF_y. \quad (25)$$

This new equation set (23), (24) and (25) can be implemented and solved in *Matlab*. The right hand sides of these equations will be further denoted with f_p, f_x and f_y, giving the shorter notation of the equation set:

$$\begin{cases} \frac{\partial p}{\partial t} & = f_p, \\ \frac{\partial w_x}{\partial t} & = f_x, \\ \frac{\partial w_y}{\partial t} & = f_y. \end{cases} \quad (26)$$

6.1 Spatial grid

In order to numerically implement these equations, a spatially centered and time centered finite-difference grid is considered. First, the spatially centered finite-difference grid is explained (see figure 2). The grid intervals of the node points are Δx and Δy. In order to get an equally spaced grid, they are held equivalent to each other. $\Delta h (= \Delta x = \Delta y)$ is defined to be the grid-spacing.

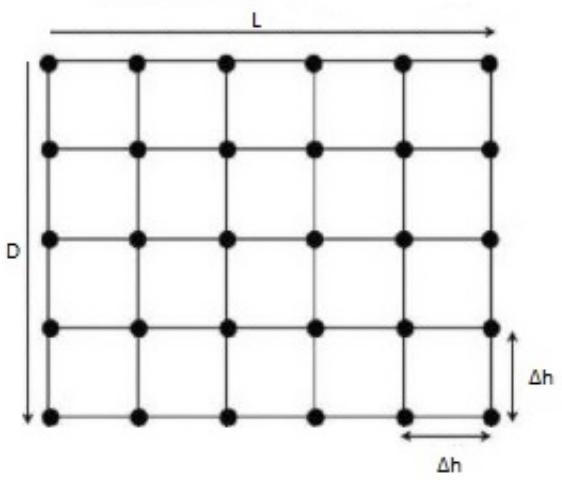

Figure 2: Spatial grid.

To simulate an intersection of the ocean, a certain length L (corresponding to the x-axis) and a depth D (corresponding to the y-axis, positively downward) are fixed. Therefore point (0,0) corresponds to the top left of the grid, laying on the surface of the ocean. The grid itself becomes:

$$\begin{cases} x_i = i \cdot \Delta h & (i = 0, 1, ..., \lfloor L/\Delta h \rfloor), \\ y_j = j \cdot \Delta h & (j = 0, 1, ..., \lfloor D/\Delta h \rfloor). \end{cases} \quad (27)$$

All the variables in equation set (23)-(25) are stored at the these node points. The density and the seismic velocity are presumed to be constant, therefore the ambient quantities: adiabatic bulk modulus ($\kappa = \varrho c^2$) and the mass buoyancy ($b = 1/\varrho$) are also constant throughout the grid.

Because the constants are constant throughout the grid, there are no boundary conditions for these parameters (they are all constant throughout the whole grid). But for the parameters that vary throughout the grid, the boundary conditions need to be stated. Because it is assumed that a lot of grid points need to be taken in order to get reliable solutions and to avoid unnecessary complications, the parameters at the boundaries of the grid are assumed to be equivalent to their interior point directly beside it. Therefore, the variables at the perimeter of the grid are calculated by equaling the variables beside it (which is the perimeter of the grid where the surrounding grid points are being removed).

6.2 Advancing in time

To advance the solution in time, a time grid has to be made. By fixing the time steps Δt and a certain end time T, the following one dimensional time grid is constructed:

$$t_k = k \cdot \Delta t \qquad (k = 0, 1, ..., \lfloor T/\Delta t \rfloor). \tag{28}$$

Next, equation (26) is of importance. A time centered finite-difference grid over two time steps is considered, resulting in the following approximations for the pressure and the acoustic velocity components:

$$\frac{\partial p}{\partial t}(i\Delta x, j\Delta y, (l+1)\Delta t) \approx \frac{p(i\Delta x, j\Delta y, (l+2)\Delta t) - p(i\Delta x, j\Delta y, l\Delta t)}{2\Delta t}, \tag{29}$$

$$\frac{\partial w_x}{\partial t}(i\Delta x, j\Delta y, (l+1)\Delta t) \approx \frac{w_x(i\Delta x, j\Delta y, (l+2)\Delta t) - w_x(i\Delta x, j\Delta y, l\Delta t)}{2\Delta t}, \tag{30}$$

$$\frac{\partial w_y}{\partial t}(i\Delta x, j\Delta y, (l+1)\Delta t) \approx \frac{w_y(i\Delta x, j\Delta y, (l+2)\Delta t) - w_y(i\Delta x, j\Delta y, l\Delta t)}{2\Delta t}, \tag{31}$$

If the errors are taken into account, the equations (29)-(31) plus their errors would become equivalence relations. This will be discussed later on in this study. For now, the errors are neglected so the approximations (29)-(31) are assumed to be equivalence relations. The implementation of the model in *Matlab* can therefore be continued.

Based on the equation (29), and taking the right hand sides of equation (26) into account, the pressure updating equation becomes:

$$p(i\Delta x, j\Delta y, (l+2)\Delta t) = p(i\Delta x, j\Delta y, l\Delta t) + 2\Delta t \cdot f_p(i\Delta x, j\Delta y, (l+1)\Delta t). \tag{32}$$

The derivatives of w_x, w_y follow similarly out of (30) and (31), resulting in the following acoustic velocity updating functions:

$$\begin{aligned} &w_x(i\Delta x, j\Delta y, (l+2)\Delta t) \\ &= w_x(i\Delta x, j\Delta y, l\Delta t) + 2\Delta t \cdot f_x(i\Delta x, j\Delta y, (l+1)\Delta t) \end{aligned}, \tag{33}$$

$$\begin{aligned} &w_y(i\Delta x, j\Delta y, (l+2)\Delta t) \\ &= w_y(i\Delta x, j\Delta y, l\Delta t) + 2\Delta t \cdot f_y(i\Delta x, j\Delta y, (l+1)\Delta t) \end{aligned}. \tag{34}$$

This updating scheme ((32). (33) and (34)) is called the non-staggered leapfrog scheme. An advantage of this scheme (in comparison with the staggered leapfrog scheme) is that it avoids the problems that arise when the variables at the half integer time steps need to be determined. The main disadvantage of this scheme is that the variables at all the grid points need to be stored over two time steps.

Out of the time-updating functions (32)-(34), it follows directly that there are some begin-conditions that need to be known in order to roll through time. The pressure and the acoustic velocity need to be known in the first two time steps, in order to calculate the third one. It is stated that their values in the first step is the same as their value in the second step, giving the following begin conditions:

$$\begin{cases} p(i\Delta x, j\Delta y, \Delta t) = p(i\Delta x, j\Delta y, 0) = p_b & \forall i, j \\ w_x(i\Delta x, j\Delta y, \Delta t) = w_x(i\Delta x, j\Delta y, 0) = 0 & \forall i, j \\ w_y(i\Delta x, j\Delta y, \Delta t) = w_y(i\Delta x, j\Delta y, 0) = 0 & \forall i, j \end{cases} \tag{35}$$

The begin values of the acoustic velocity components are set to be 0, because it is assumed that the seismic wave starts moving through the medium at time $t_0 > 0$. Without the presence of a propagating wave, there is no acoustic velocity. The pressure on the other hand can be set on any begin value p_b. Note that the updating functions are only influenced by changes in pressure, so the value of a constant background pressure throughout the grid does not affect the solution.

6.3 Source simulation

The sound wave source that creates seismic waves that will propagate through the medium is assumed to be at location (x_s, y_s). The aim is to simulate a point-source at this location. Therefore the following equation is used:

$$Q(x, y, t) = q(t)\delta(x - x_s)\delta(y - y_s), \tag{36}$$

where q represents a Mexican hat wavelet:

$$q(t) = \left(1 - \frac{(t - t_0)^2}{\sigma^2}\right) exp\left(\frac{-(t - t_0)^2}{2\sigma^2}\right), \tag{37}$$

where t_0 is the time at which the seismic wave is emitted (the time-shift for the wavelet), exp stands naturally for the exponential function and σ is a certain constant which can later on be determined (by investigating which value gives low numerical errors). The δ represents a Gauss-function, defined as:

$$\delta(r) = \phi \cdot exp\left(-\mu r^2\right), \tag{38}$$

where ϕ and μ are certain constants, which can be numerically tested later on as well.

Let it be clear that it doesn't matter with which constant the source is multiplied because the solution will be multiplied with that constant as well. For creating a point-source, it is therefore possible to simplify the Mexican hat wavelet and the Gauss-function and define them as is done in equations (37) and (38). This results in the following point-source:

$$\begin{aligned} &Q(x,y,t) = \\ &\phi^2\left(1-\frac{(t-t_0)^2}{\sigma^2}\right) exp\left(-\frac{(t-t_0)^2}{2\sigma^2} - \mu\cdot\left((x-x_s)^2+(y-y_s)^2\right)\right). \end{aligned} \tag{39}$$

7 Results

The results of a modeled seismic wave propagating through a homogeneous flowing ocean intersection are discussed. The inverse procedure to determine the velocity field out of the resulting data is applied and illustrated. The results will be evaluated and the difficulties when assuming a more realistic scenario (e.g. considering a heterogeneous flowing medium) will be discussed.

7.1 Propagation through a homogeneous flowing medium

Consider a homogeneous flowing intersection of the ocean (where the velocity vector is the same at every point). For a homogeneous uniformly moving medium, it is given that the ambient quantities do not depend on the position or the time. This means that the pressure p, the density ϱ and the medium velocity v are all constant throughout the medium.

With the help of the discussed model, a seismic wave propagating through this medium can be simulated. Technically this means that the pressure and the acoustic velocity vector through time can be calculated for a two-dimensional medium. For the first results, the discussed model, using the non-staggered leapfrog updating scheme, is applied on a homogeneous uniformly flowing medium using the following fixed parameters:

The size of the grid is set to $D = 500$ and $L = 3000$ with grid spacing $\Delta h = 10$. The time grid is constructed with end time $T = 0.8$ and time spacing $\Delta t = 0.001$. The force acting on the medium is neglected ($\mathbf{F} = \mathbf{0}$), the density is set to $\varrho = 1$ resulting in the same value for the buoyancy $b = 1/\varrho$. The speed

of sound in the ocean is assumed to be constant at $c = 1500$, resulting in the value for the adiabatic bulk modulus $\kappa = \varrho c^2$. The hydrophones are assumed to be at a depth of $y_h = 100$. The point source is held at the same depth as the hydrophones and in the middle of the x-axis, at location $(x_s, y_s) = (1500, 100)$ (the process can therefore be clearly illustrated), with the constant values $\sigma = 0.01$, $t_0 = 0.05$, $\phi = 10^6$ and $\mu = 0.0002$ to assign for the value $Q(x, y, t)$. The boundary conditions are stated as follows: $p_b = 0 \quad \forall i, j$. A homogeneous flowing medium is considered and therefore: $\mathbf{v} = (100, 0)$ is constant throughout the medium.

Using these given values for the parameters, the model can be run. Making an overwriting plot of the pressure at every time step results in an animation where one can see the development of the seismic wave, originating from the source and spreading through the medium. Making plots at several time values illustrates this process:

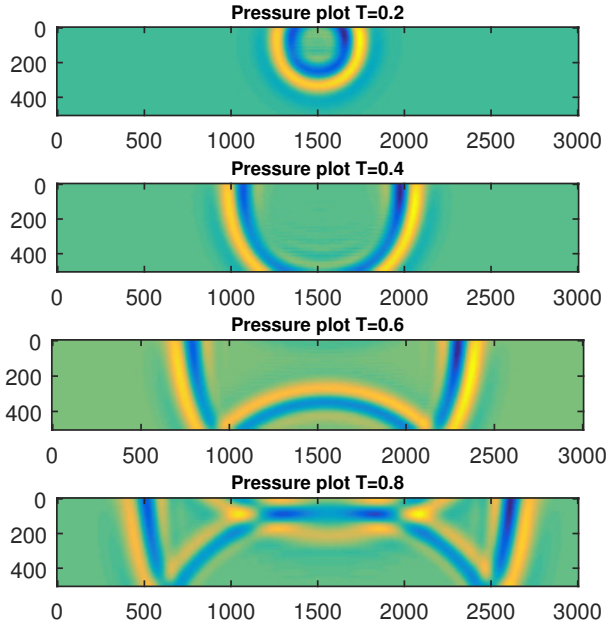

Figure 3: Pressure plots at T=0.2, T=0.4, T=0.6 and T=0.8.

In figure 3, the yellow and blue areas correspond to (relatively) high and low pressure regions. From this figure it can be seen that the emitted seismic wave propagates from the source through the medium in all directions. When the wave reaches the maximum depth (the ocean floor), the wave is reflected.

Now in order to get the data the hydrophones would receive from this wave

in this situation, the pressure is captured at the depth of the hydrophones throughout the time. This results in figure 4, where the x-axis can be seen as the horizontal line of hydrophones at their depth and the y-axis becomes the time-axis (downward means going further in time).

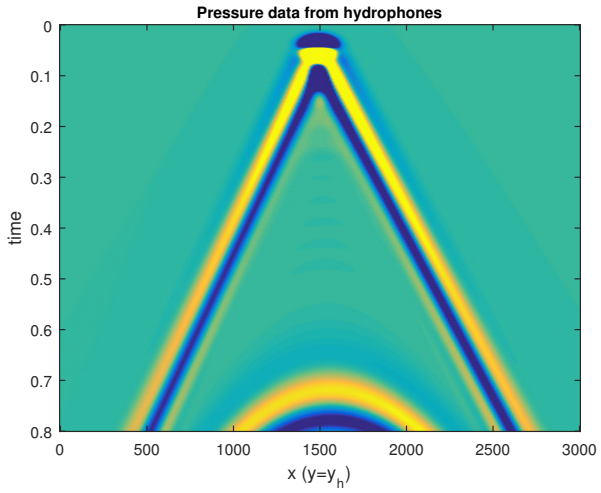

Figure 4: Pressure data from hydrophones.

The end-time in figure 4 is held at the same time as in the last plot of figure 3. Additionally, as can be seen in both figures, the reflected wave at this time $T = 0.8$ has already reached the hydrophones in the middle. Notice in figure 4 that the wave has just yet reached the hydrophone at distance $x = 500$, while it seems that the wave has already nearly passed the hydrophone at distance $x = 2500$. Even though these are both at distance 1000 from the source. The same goes for the reflected wave at distances $x = 1000$ and $x = 2000$, both 500 from the source. It appears that the seismic/pressure wave is moving faster to the right than it does to the left. This might be caused by the homogeneous velocity field $(v_x, v_y) = (100, 0)$.

This is not a coincidence. One can easily compute the pressure data from the hydrophones with a velocity field of $\mathbf{v} = (0, 0)$ (keeping all the other parameters the same) and a perfect symmetric variant of figure 4 appears (with the vertical symmetry line at $x = 1500$). When comparing both figures, it follows that indeed, the seismic wave appears to be altered more to the right due to the constant horizontal velocity field. It can be concluded that the velocity field influences the movement of the seismic wave.

So the velocity field influences the seismic wave propagating through the medium, but is it possible to determine the velocity field out of only the data from the hydrophones? Assume the data in figure 4 is the measured data from which the velocity field is unknown (this data is the synthetic measurements). The goal is to determine the velocity field out of this data. This can be achieved

by simulating the measurements for various certain velocity fields. Comparing these simulations to the data gives information about the velocity field.

But before this comparison can start, the 'measured' data and the simulated data need to be stated clearly. First the 'measured' data, or in short: data, is defined as $d(v_x^*, v_y^*)$ with its unknown velocity field $\mathbf{v}^* = (v_x^*, v_y^*)$, giving the synthetic measured data (e.g. corresponding to the data in figure 4). The measurements (at the hydrophones) can also be simulated for a given velocity field $\mathbf{v} = (v_x, v_y)$, resulting in the simulated data. The simulated data, or in short: simulation, is defined as $s(v_x, v_y)$. If the simulation is equivalent to the (measured) data ($d(\mathbf{v}^*) = s(\mathbf{v})$), the velocity field of the data is equivalent to the velocity field of the simulation ($\mathbf{v}^* = \mathbf{v}$), and thus the velocity field is determined.

Therefore, the 'difference' between the data and the simulation are of interest. Because these two components are both two-dimensional arrays (and the amount of elements are the same), they can be compared with the help of the Frobenius norm, equation (1). A function is defined for the Frobenius norm to the second power:

$$\varphi(A) := ||A||_F^2 = \sum_{i,j} (A(i,j))^2 = \sum_{i,j} (a_{ij})^2, \tag{40}$$

where A is a two dimensional array with elements a_{ij}. Therefore, if the difference between the data and the simulation is element-wise calculated, it can be put in this function giving $\varphi(d - s)$.

The data in this case is still the data as in figure 4, with end time $T = 0.8$. $\varphi(d - s(v_x, v_y))$ can be plotted for various homogeneous velocity fields : $85 \leq v_x \leq 115$ and $-15 \leq v_y \leq 15$. Making a three-dimensional plot where v_x is on the x-axis, v_y is on the y-axis and φ is on z-axis and making a contour plot results in the following two plots:

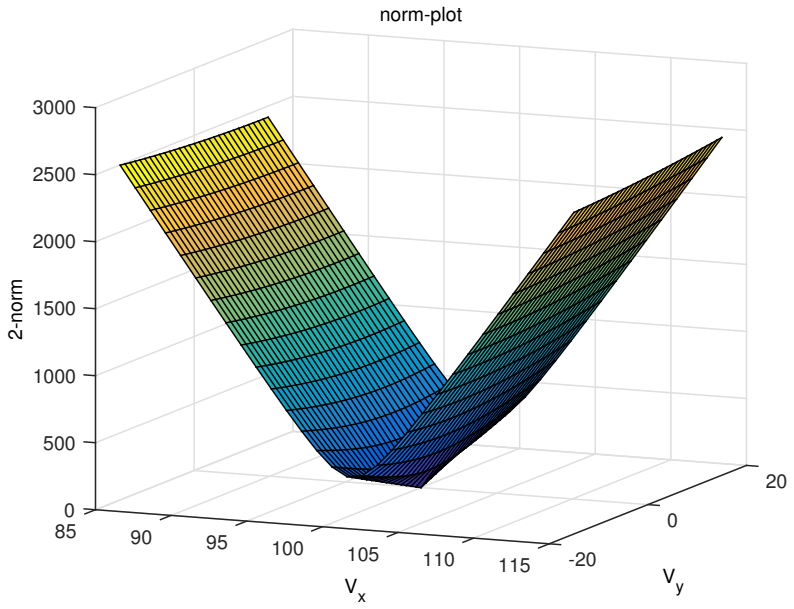

Figure 5: 3D $\varphi(d - s(v_x, v_y))$-plot.

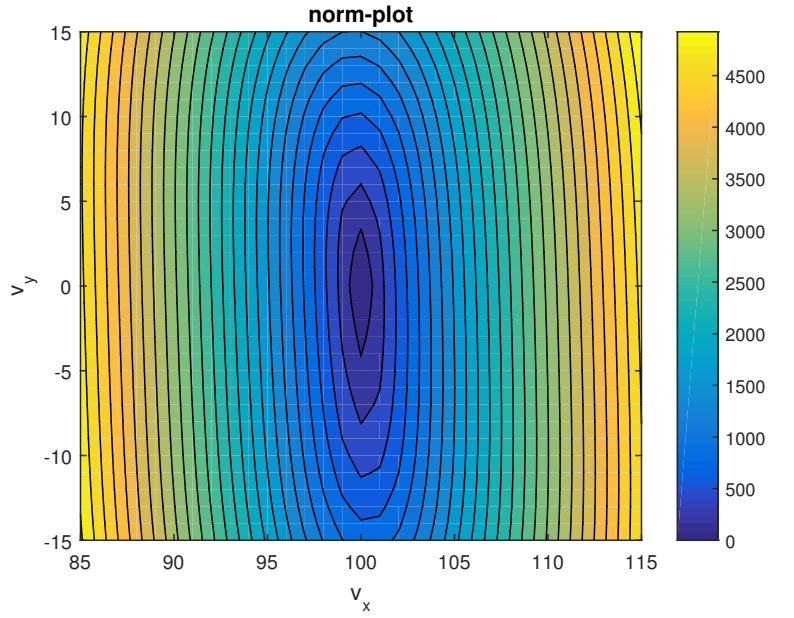

Figure 6: Contour plot $\varphi(d - s(v_x, v_y))$.

The three-dimensional figure and the contour-plot immediately show that the simulation with the (homogeneous) velocity field $\mathbf{v} = (100, 0)$ has the lowest norm value; $\varphi(d(\mathbf{v^*}) - s(100, 0)) = 0$, and $\mathbf{v^*} = (100, 0)$ is therefore a perfect prediction of what the velocity field of the measured data is. Therefore the velocity field is found out of merely the data.

Trying this same process for data at time $T = 0.6$ or earlier (again, with all the parameters held at the same values) and comparing again with the same velocity fields will not yield in the same perfect results. If this is the case, a minimum does not become clear as it is in figure 6 due to the inverse procedure needing more than merely data from the direct wave. It also needs the data from the reflected wave. This means that the reflected wave needs to have already reached some hydrophones at their horizontal line, if not, it will not be possible to determine the right velocity field out of the data.

One can also easily notice that $\varphi(d - s)$ in figure 6 is a lot more sensitive in the v_x-direction than it is in the v_y-direction. Changes in v_y result in relatively small changes in φ. It therefore appears that, by matching the simulations to the data, the horizontal velocity component is easier to extract than the vertical velocity component. This presumption is confirmed when looking at the homogeneous velocity field $\mathbf{v} = (0, 100)$. Figure 7 shows the contour plot illustrated in this situation (again, with all the parameter values held the same). Though φ appears to be more sensitive in the v_y-direction than in figure 6, φ is still more sensitive in the v_x-direction.

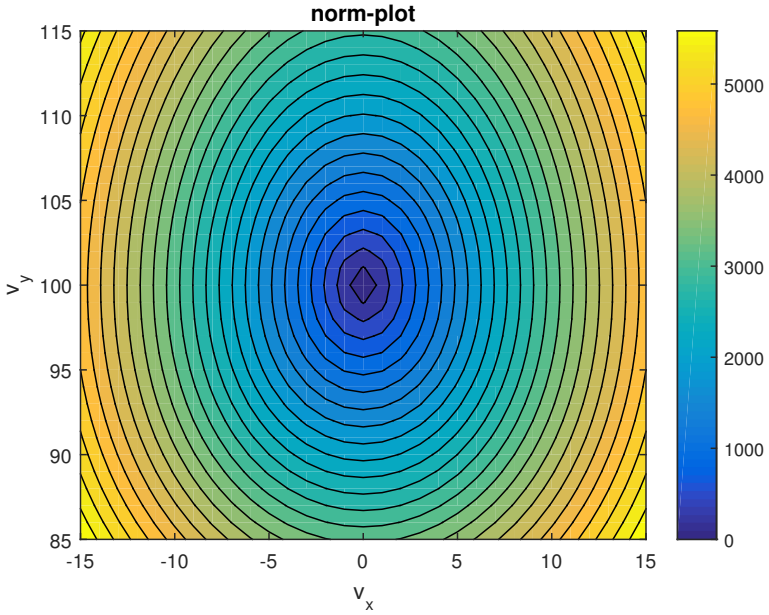

Figure 7: Contour plot $\varphi(d - s(v_x, v_y))$.

7.2 Difficulties

In the previous subsection, an ideal situation is discussed where a homogeneous flowing medium is assumed and the velocity field could be perfectly reconstructed out of the inverse procedure. Unfortunately, in most cases, it is substantially more difficult to determine the velocity field out of merely the given data. In this subsection some of these difficulties will be discussed.

In the previous subsection, the perfect choice of plotting the velocity values at $85 \leq v_x \leq 115$ and $-15 \leq v_y \leq 15$ and comparing these with the synthetic data, gave an ideal minimum in the middle with $\varphi(d-s) = 0$. Though in realistic scenarios (where a homogeneous velocity field is still assumed), one has to guess which velocity fields will probably be close to the data. It would thus take a lot more simulations to determine where this minimum lies.

Secondly, in realistic scenarios a $\varphi(d-s) = 0$ is highly unlikely. Thinking of all the approximations that are done and all the errors that were not included, the reader is referred to Appendix A for further detail. It might be more realistic if it is assumed that there is no velocity field that would simulate the measurements that would fit the data perfectly. It would then be more logical to determine the simulation with velocity field $\mathbf{v}$ that would approximate the data the best. Thus to determine the minimum of $\varphi(d-s)$.

The main issue that arises, assuming that no simulation can fit the data perfectly, is to determine a minimum of the function φ, so that a simulation can be determined that would approximate the data the best. Merely checking which simulation (of the simulations that are done) has the lowest value for $\varphi(d-s)$ might not be enough. One can not exclude that there is not another (better) minimum. If this problem could be solved analytically, one could say with certainty that the found minimum is the global optimum.

But the determining the minimum of φ analytically could be somewhat difficult. This norm function depends only on the velocity field components (d is constant). Thus one needs to partial differentiate this function to its variables:

$$\frac{\partial \varphi(v_x, v_y)}{\partial v_x} = \frac{\partial \varphi(v_x, v_y)}{\partial v_y} = 0, \tag{41}$$

with $v_x, v_y \in \mathbb{R}$, and hereby the stationary points are found. But with these stationary points, one also needs to be certain that this is not a saddle point. Suppose a certain stationary point $\mathbf{v}' = (v_x', v_y')$ is found. Then one needs to check that:

$$\frac{\partial^2 \varphi}{\partial v_x^2}\frac{\partial^2 \varphi}{\partial v_y^2} - \left(\frac{\partial^2 \varphi}{\partial v_x \partial v_y}\right)^2 > 0, \tag{42}$$

at (v_x', v_y'), which is the condition for a relative minimum or maximum. With the extra check of:

$$\frac{\partial^2 \varphi}{\partial v_x^2}(v_x', v_y') > 0, \qquad \frac{\partial^2 \varphi}{\partial v_y^2}(v_x', v_y') > 0, \tag{43}$$

one can say with certainty that (v_x', v_y') is a relative minimum.

The equations (42) and (43) are derived from Taylor's theorem for a function of two variables. After some algebra, it can be converted into these equations. The reader is referred to [Stewart, 2015] for further detail and background of equations (42) and (43).

So for a somewhat more realistic scenario (where $\varphi(d - s(v_x, v_y)) > 0 \; \forall v_x, v_y$ with $v_x, v_y \in \mathbb{R}$), the problem becomes a lot more difficult, because all these derivatives are not so easy to determine. It can therefore be concluded that in the case of a more realistic homogeneous flowing medium, the problem gets more complicated.

Now suppose a heterogeneous flowing medium is considered, where the velocity is not constant throughout the medium, but depends on the position in the grid. Therefore v_x and v_y are functions of x and y. This can also be implemented in the model and the same steps as in the homogeneous flowing medium can be followed. The seismic wave and the resulting pressure data at the hydrophones are simulated in the same way. However, the inverse procedure to determine the velocity field gets even more difficult.

Because the velocity can now vary throughout the medium, one has to estimate what the velocity is at every point in the medium to make a simulation, which magnifies the problem. Assume a certain velocity field (v_x, v_y) is chosen. The resulting simulation should then be compared with the data. The norm function $\varphi(d - s(v_x, v_y))$ can be used again to quantify the difference, but in this case, if this difference is unacceptably high, one can not easily know at what point in the grid the velocity should be changed (and to what value it should be changed) to make it a better simulation. The only thing one can do is changing the velocity field and calculating the $\varphi(d - s(v_x, v_y))$ again to check whether this gives lower values. Where in the homogeneous case, the choice of the velocity fields for the simulations can be somewhat narrowed down (v_x, v_y are known to be constant), in the heterogeneous case, this choice seems to be completely random.

Thus it can be concluded that for a heterogeneous case, the problem gets a lot more complicated. Though if a specific state of the heterogeneous flowing field is assumed (like for example a stratified moving medium, the reader is referred to [Winters and Rouseff, 1993]) or if the problem is simplified elsewhere (the reader is referred to [Rouseff and Winters, 1994]), for a realistic heterogeneous case, this is still an undetermined problem.

8 Conclusion

Seismic oceanography investigates structures within the interior of the ocean. This includes trying to determine the velocity field by means of sound waves. Considering a two-dimensional intersection of the ocean, a sound wave propagating through this medium can be modeled, including the reflection from the ocean floor. By means of calculating the pressure throughout this grid, throughout the time, the propagating wave can be simulated.

Measurements done at certain observing points can be simulated by keeping record of the pressure throughout the time at that location. Assuming 'real' measurements are done and these records with an unknown velocity field are known, the question would be how to figure out the velocity field.

Assuming this unknown velocity field is a homogeneous flowing medium, simulations can be done for various homogeneous velocity fields to determine what measurements would be recorded at the observing points. By comparing all these simulated records to the 'real' measurements, the simulation that has its records closest to the real records has a velocity field that approximates the real situation the best.

This inverse procedure theoretically works for an ideal situation where a homogeneous velocity field is considered. Thus, one can argue that it is possible to determine the velocity field out of the observance of seismic waves. Though it seems that, even in ideal conditions, the horizontal velocity component can be extracted more easily than the vertical velocity component. Therefore, it is not unthinkable that in other situations, the vertical velocity component can not be accurately predicted.

If some more realistic constraints are adopted, applying the inverse procedure becomes a lot more difficult. Assuming that no simulation can fit the measured data perfectly makes it theoretically a lot more challenging. And for assuming certain heterogeneous media (like turbulent media), this is even an undetermined problem.

A Appendix : stability and accuracy

There are 3 kind of errors that can occur in the discussed model: numerical errors (including the spatial derivative error and the time derivative error), the error on the data and the error in calculating the derivative of the function $\varphi = ||data - sim||_F^2$.

A.1 Numerical errors

First, the numerical errors are discussed. The approximations (29)-(31) used for the updating equations in the model can also be represented with their errors. These are the time derivative errors.

So in order to calculate the error of the derivative of the pressure function (29), theorem 2.1 needs to be applied. First the approximation which was used is stated again:

$$\frac{\partial p}{\partial t}(i\Delta x, j\Delta y, (l+1)\Delta t) \approx \frac{p(i\Delta x, j\Delta y, (l+2)\Delta t) - p(i\Delta x, j\Delta y, l\Delta t)}{2\Delta t}. \quad (44)$$

For both components $p(i\Delta x, j\Delta y, (l+2)\Delta t)$ and $p(i\Delta x, j\Delta y, l\Delta t)$, a second-order Taylor polynomial is taken. The coordinates of the pressure are always the same in this equation, so the components are shortened for convenience to $p((l+2)\Delta t))$ and $p(l\Delta t)$ (for every possible i and j). This gives:

$$p((l+2)\Delta t) = p((l+1)\Delta t) + \Delta t \cdot p'((l+1)\Delta t) + \frac{(\Delta t)^2}{2} p''((l+1)\Delta t) + \frac{(\Delta t)^3}{6} p'''(\xi_1),$$

and

$$p(l\Delta t) = p((l+1)\Delta t) - \Delta t \cdot p'((l+1)\Delta t) + \frac{(\Delta t)^2}{2} p''((l+1)\Delta t) - \frac{(\Delta t)^3}{6} p'''(\xi_2),$$

where $\xi_1 \in](l+1)\Delta t, (l+2)\Delta t[$, $\xi_2 \in]l\Delta t, (l+1)\Delta t[$ and the derivatives of p stand for the derivatives with respect to the time. Implementing these in equation (44) gives:

$$\frac{\partial p}{\partial t}((l+1)\Delta t) = p'((l+1)\Delta t) + \frac{(\Delta t)^2}{12}\left(p'''(\xi_1) + p'''(\xi_2)\right), \quad (45)$$

with the help of the intermediate value theorem, $(p'''(\xi_1) + p'''(\xi_2))$ can be shortened to $2p'''(\xi)$ for some $\xi \in [\xi_1, \xi_2]$, assuming that p''' is a continuous function. Thus the time derivative error (defined by τ) of the pressure updating function is given by:

$$\tau = \frac{(\Delta t)^2}{6} p'''(\xi). \quad (46)$$

with some $\xi \in]l\Delta t, (l+2)\Delta t[$.

The time derivative errors of the updating functions of w_x, w_y follow similarly out of their derivative functions (30) and (31), giving the same error as

in equation (46). But instead of p''', the third derivative w_x and w_y is applied. To determine the order of the total error at the end time caused by these approximation errors in each separate step, one can multiply this error with the amount of steps that are needed.

The second numerical error that occurs is the spatial derivative error. In equations (23)-(25) the derivative of the pressure and the acoustic velocity components with respect to x and y need to be known in order to progress through time. These derivative functions are calculated in the model with the help of the gradient function in *Matlab*. This gradient function calculates the gradient of a matrix, giving two whole matrices back (one for the derivative with respect to x, and one for the derivative with respect to y), both with the same amount of elements as the original matrix.

The gradient function uses the central difference method for interior data points and the single-sided difference method for the edges of the matrix. Because the amount of grid points are assumed to be very high, the gradient of the boundaries can be neglected (the value for an edge can for example be assumed to be equivalent to a calculated point beside it). Therefore, the single-sided difference method is ignored.

The derivative of the pressure with respect to x, by means of the central difference method, is calculated as follows:

$$\frac{\partial p}{\partial x}(i\Delta x, j\Delta y) \approx \frac{p((i+1)\Delta x, j\Delta y) - p((i-1)\Delta x, j\Delta y)}{2\Delta x}, \tag{47}$$

$\forall 1 \leq i \leq (\lfloor L/\Delta h \rfloor - 1)$, $\forall 0 \leq j \leq \lfloor D/\Delta h \rfloor$, thus for all the interior points. The process of calculating the spatial derivative error goes equivalent to the process of calculating the time derivative error. The second order Taylor polynomial is taken of $p((i+1)\Delta x, j\Delta y)$ and $p((i-1)\Delta x, j\Delta y)$, and after some algebra, the resulting error becomes:

$$\tau = \frac{(\Delta x)^2}{6} p'''(\xi), \tag{48}$$

with some $\xi \in](i-1)\Delta x, (i+1)\Delta x[$ and where p''' stands in this case of course for the third derivative of p with respect to x.

The spatial derivative error is shown for the derivative of the pressure with respect to x. And because the same method is used for the spatial derivative with respect to y (replacing the Δx with Δy and so on), this process goes exactly similar for the derivative of the pressure with respect to y. Note that $\Delta h = \Delta x = \Delta y$ still counts if an equally spaced grid is considered.

The whole process for determining the spatial derivative errors of the acoustic velocity components (the derivatives of both components with respect to x and y) goes exactly the same. Therefore, all the spatial derivative errors can be calculated in a similar way as is demonstrated above.

A.2 Error on the data

In practice, it is highly probable that there is noise on the measured data. Noise on the data can for example be defined as η, giving the new data function $d_{new} := d(\mathbf{v}^*) + \eta$. This can trouble the inverse procedure if the η is relatively big, which may yield in velocity fields which do not correspond with reliable solutions (which are not close to $\mathbf{v}^*$). It is imaginable that it is extremely hard to find a reliable velocity field if only d_{new} is known and η is unknown but known to be big.

A.3 Derivative of the norm-function φ

And thirdly, if the derivative of the function φ needs to be evaluated to find a minimum for $\varphi(d - s(v_x, v_y))$, and this derivative is numerically approached, the error in the derivative function needs to be included. Depending on how this function is numerically calculated, this error needs to be accounted for.

References

[Holbrook et al., 2003] Holbrook, W. S., Páramo, P., Pearse, S., and Schmitt, R. W. (2003). Thermohaline fine structure in an oceanographic front from seismic reflection profiling. *Science*, 301(5634):821–824.

[Landau and Sykes, 1987] Landau, L. D. and Sykes, J. (1987). Fluid mechanics: Vol 6.

[Ostashev, 1987] Ostashev, V. (1987). on sound wave propagation in a three-dimensional inhomogeneous moving medium. *Diffraction and Wave Propagation in Inhomogeneous Media*, pages 42–49.

[Ostashev et al., 2005] Ostashev, V. E., Wilson, D. K., Liu, L., Aldridge, D. F., Symons, N. P., and Marlin, D. (2005). Equations for finite-difference, time-domain simulation of sound propagation in moving inhomogeneous media and numerical implementation. *The Journal of the Acoustical Society of America*, 117(2):503–517.

[Rouseff and Winters, 1994] Rouseff, D. and Winters, K. (1994). Two-dimensional vector flow inversion by diffraction tomography. *Inverse Problems*, 10(3):687.

[Ruddick et al., 2009] Ruddick, B., Song, H., Dong, C., and Pinheiro, L. (2009). Water column seismic images as maps of temperature gradient. *Oceanography*, 22(1):192.

[Stewart, 2015] Stewart, J. (2015). *Calculus: early transcendentals*. Cengage Learning.

[Vuik et al., 2006] Vuik, C., van Beek, P., Vermolen, F., and van Kan, J. (2006). *Numerieke methoden voor differentiaalvergelijkingen*, volume 159. VSSD.

[Winters and Rouseff, 1993] Winters, K. B. and Rouseff, D. (1993). Tomographic reconstruction of stratified fluid flow. *Ultrasonics, Ferroelectrics, and Frequency Control, IEEE Transactions on*, 40(1):26–33.